ABUAD Journal of Engineering Research and Development (AJERD)
ISSN (online): 2645-2685; ISSN (print): 2756-6811

Volume 7, Issue 2, 425-435

Three-State Hidden Markov Model for Spectrum Prediction in Cognitive Radio Networks

Emmanuel Oluwatosin RABIU [1], Damilare Oluwole AKANDE[1], Zachaeus Kayode ADEYEMO[1], Isaac Akinwale AKANBI[2], Oluwole Oladele OBANISOLA[3]

[1]*Electronic and Electrical Engineering Department, Ladoke Akintola University of Technology, Ogbomosho, Nigeria*
oluwatosin.rabiu@gmail.com/doakande@lautech.edu.ng/zkadeyemo@lautech.edu.ng

[2]*Nigerian Communications Commission, Abuja, Nigeria*
engrakanbiia@gmail.com

[3]*Department of Electrical and Electronic Engineering, Ajayi Crowther University, Oyo, Nigeria*
oo.obanisola@acu.edu.ng

Corresponding Author: doakande@lautech.edu.ng, +2348066133011
Date Submitted: 17/07/2024
Date Accepted: 08/10/2024
Date Published: 13/10/2024

Abstract: *The exponential growth and proliferation of wireless devices for different wireless applications have led to the emergence of cognitive radio network (CRN) for optimal utilization of scarce spectrum resources. However, these resources have grossly been under-utilized due to the inaccurate spectrum predictions. Existing spectrum occupancy and prediction techniques which rely on 2-state hidden Markov model (HMM) results in false alarm or missed detection caused by noisy or incomplete observable effects. In this paper, a 3-state HMM spectrum occupancy and prediction technique in CRNs is proposed. The transmission, emission and initial state probabilities of the proposed 3-state HMM parameters were derived based on the three canonical problems associated with HMM. The evaluation, decoding and learning problems were solved using Forward algorithm, Viterbi algorithm and the Baum-Welch algorithm, respectively. The performance of the proposed 3-state HMM spectrum prediction technique was evaluated using prediction accuracy, probability of detection and spectrum utilization efficiency. The simulation results obtained revealed that the 3-state HMM outperformed the 2-state HMM spectrum prediction technique by 24.1% in prediction accuracy.*

Keywords: *Cognitive Radio Network, 3-state HMM, Spectrum Prediction, Prediction Accuracy, Probability of Detection*

1. INTRODUCTION

A remarkable success recorded over the decade by the wireless communication research community is the tremendous and evolutionary transformation from the first generation (1G) cellular telephone systems to the fifth generation (5G) network [1-3]. Spectrum is an important component of wireless communication and has been reported to be scarce and under-utilized because of different emerging wireless applications. To subdue the challenge of spectrum scarcity, cognitive radio network (CRN) was introduced by Mitola in [4] as one of the important components of the 5G network. The technology helps to increase spectral efficiency as secondary users (SUs) or cognitive radio (CR) users are allowed to access spectrum holes left unused by licensed or primary users (PUs) [5,6]. In order to avoid undue interference to licensed users, there is need for a dynamic spectrum access (DSA) by cognitive radio nodes which require algorithms and protocols for rapid spectrum sensing accuracy, efficient coordination and beneficial cooperation [7-9].

Spectrum prediction is a robust technique complimentary to spectrum sensing for obtaining the relevant information as regards spectral evolution. It also provides identification of spectrum holes as a band of frequencies meant for a certain PU but which are found vacant at some points in time and specific geographic locations [10]. Spectrum sensing involves the determination of the spectrum state in a passive manner using various signal detection methods. Spectrum prediction on the other hand detects the state of radio spectrum from already known spectrum occupancy statistics by effectively utilizing the existing inherent correlations in a proactive manner [11-13]. Spectrum prediction involved different techniques ranging from pure lookup table (LUT) to advanced techniques such as evolutionary algorithms, artificial neural network (ANN), hidden Markov model (HMM) and machine learning (ML) among others. Generally, all spectrum prediction techniques have been categorized into regression analysis-based, machine learning-based and Markov model-based [14-17].

Some of the existing contributions are discussed therein. In the work presented in [18], the design of a spectrum prediction technique using a neural network based and hidden Markov model which is a combination of a regression analysis, and a Markov model was performed. However, the work considered only two physical channel statuses which are

busy state and idle state. ML techniques of both ANN and support vector machine (SVM) were employed in [19] for spectrum prediction of future inactive times.

In [20], a 2-state HMM to predict channel activity patterns through a cyclic process for realizing the real parameter of channel usage was applied. The 2-state channels of active and inactive states were considered in slow, balanced and heavy traffic scenarios for checking the prediction outcomes. A hybrid of Bayesian theorem and exponential weighted moving average (EWMA) which is a regression analysis-based spectrum prediction was proposed by Jaison et al. [21]. The work utilized the conditional probability involving previous states to predict the next state.

An adaptive neuro fuzzy interference system (ANFIS) was proposed in [5] using regression analysis-based artificial neural networks and rule based fuzzy inference system for spectrum availability prediction in CRNs. Previous works such as [20] and [12] which utilized ML techniques show decrease in speed and suffers inaccuracy when large scale data sets were involved. On the other hand, regression analysis-based spectrum prediction techniques proposed in [21] suffered performance loss and difficulty in updating the regressive coefficient because of high complexity. The HMM techniques have shown a good spectrum prediction accuracy and are widely used because of its ability to simulate complex sequence of data sources as well as its consideration of historical information [13,23].

In [24], an HMM-based spectrum prediction algorithm for industrial applications with capability of predicting future multiple slots by formulating the prediction problem as a maximum likelihood (MLH) classification approach was proposed. Consideration was given to a higher number of hidden states which gave excessive increase in misclassification error due to model over-fitting of LUT employed and accompanied longer transmission delays. The prediction of channel state for cognitive radio using higher-order HMM (HO-HMM) was presented in [25] which considered more than one historical state for prediction of future states with unbearable increased complexity.

In view of the existing contributions, it is evidently clear that the accurate prediction of the channel state still possesses a major problem to CRN and require further consideration for efficient spectrum utilization and resource management. In this paper, the main contribution is to accurately predict the channel state of CRNs using the 3-state HMM for better utilization of the spectrum with less complexity and reduction of interference to PU transmission. Also, the prediction accuracy (PA), probability of detection (PD) and spectrum utilization efficiency (SUE) evaluation of the technique was performed and compared with a 2-state HMM technique.

The paper is structured as follows: section II presents the system model, and the 3-state HMM formulation. In section III, the proposed 3-state spectrum occupancy and prediction is presented. In section IV, we presented the numerical results and discussions. Section V concludes the paper.

2. SYSTEM MODEL AND THREE-STATE HMM FORMULATION

2.1 System Model

In this paper, *fuzzy* state was introduced to enhance the 2-state spectrum prediction models in CRNs using HMM. The 2-state HMM largely presumed the PU networks to be either in a *busy* or *idle* state. The 3-state HMM prediction technique depicted in Figure 1 is based on the SU spectrum sensing outcome which is dependent on the true outcome of the PU transmission activities.

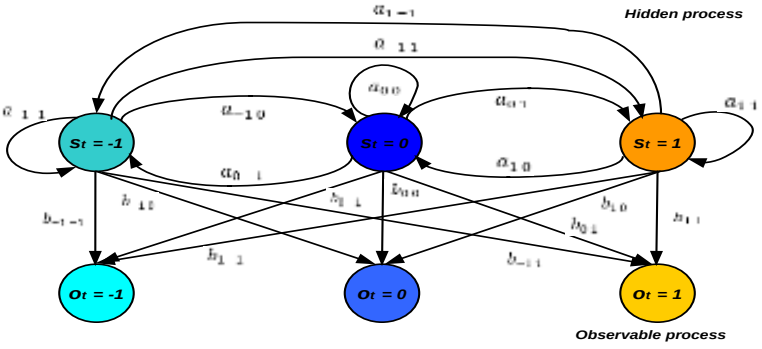

Figure 1: 3-State Hidden Markov Model

An additional state named *fuzzy* is introduced in this paper to enhance the 2-state HMM spectrum prediction model with the PU network which can either be in a *busy* or *idle* state. The 3-state HMM also comprises parameters: initial state probability vector, transmission probability distribution and emission probability distribution.

2.2 Spectrum sensing of the 3-state HMM

The signal received by a PU receiver $'y_{PU-RX}(t)'$ from the PU transmitter $'PU-TX'$ is written as.

$$y_{PU-RX}(t) = s_{PU-TX}(t)\, x_{PU-TX}(t) + w_{PU}(t) \quad (1)$$

where,
$s_{PU-TX}(t)$ is the PU state,

$x_{PU-TX}(t)$ is the signal originating from the PU transmitter and
$w_{PU}(t)$ is the additive Gaussian white noise modelled as $\mathcal{W}\sim(0,\sigma^2)$.

The spectrum sensing technique used at the SU is the energy detector which is based on the comparison of the received signal energy and the decision threshold $'\lambda_{th}'$ that is characterized with low computational complexities [8,26]. Consequently, due to the additional state the third hypothesis was included alongside that of the 2-state as shown the Figure 1 which are characterized with noise and channel impairments and result in observable errors.

It is worth mentioning that the purpose of the *fuzzy* state is to minimize the interruption of the PU transmission which results in interference. This helps to restrict the SUs from opportunistically accessing the channel when the condition is not fully known. Equation (1) is then modified to accommodate the third state and is obtained using the Venn diagram concept as depicted in Figure 2 with the conditions expressed in (2) as.

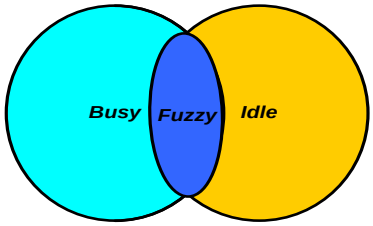

Figure 2: Venn diagram representation of the 3-state

$$y(t)=\begin{cases} w(t), & \big(s(t)x(t)\cup w(t)\big)\cap w(t) \rightarrow idle \\ s(t)x(t)+w(t)= \begin{cases} \big(s(t)x(t)\cup w(t)\big)\cap s(t)x(t), \rightarrow busy \\ s(t)x(t)\cap w(t), \rightarrow fuzzy \end{cases} \end{cases} \tag{2}$$

Therefore, the hypothesis deduced in (2) is obtained as.

$$\begin{aligned} H_{-1}&: -1 \rightarrow PU\ transmission\ \ unknown\ (fuzzy) \\ H_0&: \ \ 0 \ \rightarrow PU\ transmission\ \ absent\ (idle) \\ H_1&: \ \ 1 \ \rightarrow PU\ transmission\ \ present\ (busy) \end{aligned} \tag{3}$$

The spectrum sensing of the 3-state HMM prediction technique is characterized with the state space $S=\{-1,0,1\}$ and emission space $O=\{-1,0,1\}$.

2.3 Formulation of 3-state HMM

Consider the 3-state HMM, each state ($S=s_1,s_2,s_3,\dots,s_T$) produces a number of outputs with a unique probability distribution and every distinct output is generated at any state. This approach involves a hidden process ($s_t\in S$) and an observable process ($O=o_1,o_2,o_3,\dots o_T$) both making up a doubly stochastic process which allows observation symbols to be emitted from each state with a finite probability distribution. The emission probability matrix ($\boldsymbol{B}$) in each state is the probability that symbol (v_k) is emitted in state s_j. The proposed approach makes it possible for a channel to transit to any state in a single transition process as illustrated. The 3-state HMM is expressed according to [24] as.

$$\lambda = (\pi,\boldsymbol{A},\boldsymbol{B}) \tag{4}$$

where,
π is the initial state probability distribution for the 3-state HMM written as.

$$\pi = [\pi_{-1}\ \pi_0\ \pi_1] = [P(s_t=-1)\ P(s_t=0)\ P(s_t=1)] \tag{5}$$

Equation (5) can be further expressed as.

$$\pi = \left[\frac{a_{-1\,0}+a_{-1\,1}}{a_{-1\,0}+a_{-1\,1}+a_{0\,-1}+a_{1\,-1}} \quad \frac{a_{0\,-1}+a_{0\,1}}{a_{0\,-1}+a_{0\,1}+a_{-1\,0}+a_{1\,0}} \quad \frac{a_{1\,-1}+a_{1\,0}}{a_{1\,-1}+a_{1\,0}+a_{0\,1}+a_{-1\,1}}\right] \tag{6}$$

where,
$a_{ij}\in\boldsymbol{A}$ is the element of the state transition probability distribution matrix when traversing between state i and state j.
The addition of the initial state probabilities of each state is given as.

$$\sum_{i=1}^{3}\pi_i = 1 \tag{7}$$

The state transition probability distribution of a n-state HMM is expressed as.

$$a_{ij} = P(q_{t+1} = s_j | q_t = s_i),\ \forall\ 1 \le i,j \le n \tag{8}$$

In this paper, a 3-state HMM with the state transition matrix ($\boldsymbol{A}$) with $n \times n$ dimension is expressed as.

$$\boldsymbol{A} = \begin{bmatrix} P(s_j = -1|s_i = -1) & P(s_j = -1|s_i = 0) & P(s_j = -1|s_i = 1) \\ P(s_j = 0|s_i = -1) & P(s_j = 1|s_i = 0) & P(s_j = 0|s_i = 1) \\ P(s_j = 1|s_i = -1) & P(s_j = 1|s_i = 0) & P(s_j = 1|s_i = 1) \end{bmatrix} = \begin{bmatrix} a_{-1\,-1} & a_{-1\,0} & a_{-1\,1} \\ a_{0\,-1} & a_{0\,0} & a_{0\,1} \\ a_{1-1} & a_{1\,0} & a_{1\,1} \end{bmatrix} \tag{9}$$

and the sum of the traversing path probabilities is given as.

$$\sum_{j=1}^{3} a_{ij} = 1, \quad 0 \le a_{ij} \le 1 \tag{10}$$

Likewise, the emmision or observation probabilities distribution for the 3-state HMM is expressed as.

$$b_{jk} = P(o_k|q_{t+1} = s_j),\ \forall\ 1 \le j \le n,\ \forall\ 1 \le k \le m \tag{11}$$

this can be further used to form a $n \times m$ observation matrix ($\boldsymbol{B}$) expressed as.

$$\boldsymbol{B} = \begin{bmatrix} P(o_k = -1|s_j = -1) & P(o_k = -1|s_j = 0) & P(o_k = -1|s_j = 1) \\ P(o_k = 0|s_j = -1) & P(o_k = 1|s_j = 0) & P(o_k = 0|s_j = 1) \\ P(o_k = 1|s_j = -1) & P(o_k = 1|s_j = 0) & P(o_k = 1|s_j = 1) \end{bmatrix} = \begin{bmatrix} b_{-1\,-1} & b_{-1\,0} & b_{-1\,1} \\ b_{0\,-1} & b_{0\,0} & b_{0\,1} \\ b_{1-1} & b_{1\,0} & b_{1\,1} \end{bmatrix} \tag{12}$$

and the sum of the emission probabilities of each state is given as.

$$\sum_{k=1}^{3} b_{jk} = 1, \quad 0 \le b_{jk} \le 1 \tag{13}$$

The observable states within the emission sequence are conditionally independent of the state sequence by applying the first order Markov assumption and Markovian property [23] which is expressed as.

$$f_{o_t|s_t,o_{t-1}}(o_t|s_t, o_{t-1}) = f_{O|S}(o_t|s_t) \tag{14}$$

Therefore, expressions for the emission probabilities in (12) are written as.

$$b_{-1\,-1} = 1 - b_{-1\,0} - b_{-1\,1} \tag{15a}$$
$$b_{0\,0} = 1 - b_{-1\,0} - b_{1\,0} \tag{15b}$$
$$b_{1\,1} = Q_{\mu}(\sqrt{2\gamma}\sqrt{\lambda}) \tag{15c}$$
$$b_{-1\,0} = b_{0\,-1} = 1 - \frac{\Gamma(\mu,\lambda/2)}{\Gamma(\mu)} \tag{15d}$$
$$b_{0\,1} = b_{1\,0} = \frac{\Gamma(\mu,\lambda/2)}{\Gamma(\mu)} \tag{15e}$$
$$b_{-1\,1} = b_{1\,-1} = 1 - Q_{\mu}(\sqrt{2\gamma}\sqrt{\lambda}) \tag{15f}$$

where,
γ is the instanteneous SNR,
μ is the time-bandwidth function.
By assuming the symmetric property for emission probabilities in (12), Equations (15c) and (15e) correspond to PD and PFA, respectively, while others are categorized as the PM. According to [27], Equation (15c) is obtained using the generalised Marcum Q-function given as.

$$Q_z(a,\tau) = \left(\frac{1}{a^{(z-1)}}\right) \int_{\tau}^{\infty} x^z\, exp\left(-\frac{(x^2+a^2)}{2}\right) I_{(z-1)}(ax)dx \tag{16}$$

where,
$I_{(z)}$ is the modified Bessel function of the 1st order.

Similarly, Equation (15e) is obtained by using the incomplete gamma function given as;

$$\Gamma(a,x) = \int_{x}^{\infty} t^{(a-t)}\, exp(-t)dt \tag{17}$$

3. PROPOSED THREE-STATE SPECTRUM OCCUPANCY AND PREDICTION

In this section, the future state of the channel occupancy $T+1$ is determined and predicted using the previous channel state sequence at instant time T based on observation sequence experienced by the SU. Considering the proposed 3-state HMM, according to [28] the three canonical problems associated with the HMM namely: likelihood, decoding and training processes are solved for the CRN using the forward and backward algorithm, Viterbi algorithm and the Baum-Welch algorithm, respectively, given the $O = o_1, o_2, \ldots, o_T$ and λ.

Problem 1 (Likelihood): How to determine the probability that the observed sequence came from the model, $P(O|\lambda)$?

Problem 2 (Decoding): How to determine the most likely hidden state of the model that would generate the output sequence?

Problem 3 (Training): How can the λ be adjusted by training the parameters $\boldsymbol{A}$ and $\boldsymbol{B}$ in order to maximize $P(O|\lambda)$?

The solution to the three problems posed are discussed as follows:

The forward algorithm: The joint probability function is given as $\alpha_t(i) = P(o_1, o_2, \ldots, o_t,\ q_t = s_i|\lambda)$, then $\alpha_t(i)$ is calculated recursively as.

Initialization: $\alpha_1(i) = \pi_i b_i(o_1), 1 \le i \le 3$ (18)

Recursion: $\alpha_t(j) = b_j(o_t)\left[\sum_{i=1}^{3} \alpha_{t-1}(i)\, a_{ij}\right],\ 1 \le i,j \le 3,\ 2 \le t \le T$ (19)

Termination: $(O|\lambda) = \sum_{i=1}^{3} \alpha_T(i)$ (20)

The backward algorithm: The steps are similar to those of forward algorithm but the conditional probability $\beta_t(i)$ is given as $\beta_t(i) = P(o_{t+1}, o_{t+2}, \ldots, o_T|q_t = s_i, \lambda),\ 1 \le i \le 3$, then, the following procedure are employed recursively as:

Initialization: $\beta_T(i) = 1,\ 1 \le i \le 3$ (21)

Recursion: $\beta_t(i) = \sum_{j=1}^{3} a_{ij} b_j(o_{t+1}) \beta_{t+1}(j),\ 1 \le i \le 3,\ T-1 \ge t \ge 1$ (22)

Termination: $P(O|\lambda) = \sum_{j=1}^{3} \pi_i b_j(o_1) \beta_1(i),\ 1 \le i \le 3$ (23)

Since the forward algorithm is readily available to solve the first canonical problem, the computation of the backward variable $\beta_t(i)$ is important in solving other canonical problems.

The Viterbi algorithm (Decoding process): The decoding problem requires the inference of the optimal state sequence that is generated by the O given λ. The Viterbi algorithm is then employed to solve this optimization-related problem. The variable $\delta_t(i)$ is used to make known the highest probability within a path at time instant t, which accounts for the first t observations and ends in state $(s_i = q_t)$. An array $\psi_t(j)$ is introduced to recover the state sequence which keeps track of argument for maximization of $\delta_t(i)$. By using $\delta_t(i)$, the optimal state q_t^* is calculated after the most likely state q_t at time instant t and is deduced as, $q_t = arg\ max_{1 \le i \le 3}\, \delta_t(i),\ 1 \le t \le T$

Initialization: $\delta_1(i) = \pi_i b_i(o_1),\ 1 \le i \le 3$ (24)

$$\psi_1(1) = 0 \quad (25)$$

Recursion: $\delta_t(j) = max_{1 \le i \le 3}[\delta_i(t-1)\, a_{ij}|b_j(o_t)],\ 2 \le t \le T,\ 1 \le j \le 3$ (26)

$$\psi_t(j) = arg\ max_{1 \le j \le 3}\left[\delta_i(t-1)a_{ij}\right],\ 2 \le t \le T,\ 1 \le j \le 3 \quad (27)$$

Termination: $q_T^* = arg\ max_{1 \le i \le 3}\, \delta_T(i)$ (28)

Backtracking: $q_t^* = \psi_{t+1} q_{(t+1)}^*,\ t = T-1, T-2, \ldots, 1$ (29)

The Baum-Welch algorithm (Training process): To maximize the probability of the observation sequence emitted by a given state sequence $P(O|\lambda)$, the Baum-Welch algorithm is employed to adjust the parameters of the proposed model. The algorithm is used to obtain the optimal model parameters, $\lambda^* = (\pi^*, \boldsymbol{A}^*, \boldsymbol{B}^*)$, through an iterative updating process until a terminating condition is reached. Also, the probability of being in state s_i at time t and state s_j at time $t+1$ based on forward and backward variables is given as.

$$\xi_t(i,j) = P\left(q_t = s_i, q_{t+1} = s_j|O, \lambda\right) = \frac{\alpha_t(i) a_{ij} b_j(O_{t+1}) \beta_{t+1}(j)}{P(O|\lambda)} = \frac{\alpha_t(i) a_{ij} b_j(O_{t+1}) \beta_{t+1}(j)}{\sum_{i=1}^{3} \sum_{j=1}^{3} \alpha_t(i) \alpha_{ij} b_j(O_{t+1}) \beta_{t+1}(j)} \quad (30)$$

Therefore, the probability of the proposed model to be in state s_i at time instant t given as $\gamma_t(i)$ as required in the training process is expressed as.

$$\gamma_t(i) = P(q_t = s_i|O,\lambda) = \frac{\alpha_t(i)\beta_t(i)}{P(O|\lambda)} = \frac{\sum_{i=1}^{3}\beta_t(i)}{\sum_{i=1}^{3}\alpha_t(i)\beta_t(i)} \quad (31)$$

hence, Equation (31) is further expressed as.

$$\gamma_t(i) = \sum_{j=1}^{3}\xi_t(i,j) \quad (32)$$

The training process is then executed through the maximum likelihood estimator (MLE) in a step-by-step procedure as follows.
Step 1: Initialize the proposed model's parameter λ_0 and calculate $P(O|\lambda_0)$ with forward algorithm
Step 2: Calculate the optimal parameters, λ^*, for $1 \leq i \leq 3$

$$\pi_i^* = \gamma_1(i) \quad (33)$$

$$\boldsymbol{A}^* = a_{ij}^* = \frac{\sum_{t=1}^{T-1}\xi_t(i,j)}{\sum_{t=1}^{T-1}\gamma_t(i)}, 1 \leq i,j \leq 3 \quad (34)$$

$$\boldsymbol{B}^* = b_{jk}^* = \frac{\sum_{t=1,O_t=v_{k_{t=1}}}^{T}\gamma_t(j)}{\sum_{t=1}^{T}\gamma_t(j)}, 1 \leq j,k \leq 3 \quad (35)$$

Step 3: If $P(O|\lambda^*) > P(O|\lambda)$, repeat step 2. Otherwise, terminate.

Prediction decision: The prediction decision for the proposed 3-state HMM is presented in this section. The future state at time $T+1$, with observation o_{T+1} is predicted using the decision rule expressed in (36) as:

$$o_{T+1} = \begin{cases} 1, & if\ P(O,1|\lambda^*) > P(O,0|\lambda^*)\ and\ P(O,1|\lambda^*) > P(O,-1|\lambda^*) \\ 0, & if\ P(O,0|\lambda^*) > P(O,1|\lambda^*)\ and\ P(O,0|\lambda^*) > P(O,-1|\lambda^*) \\ -1, & if\ P(O,-1|\lambda^*) > P(O,0|\lambda^*)\ and\ P(O,-1|\lambda^*) > P(O,1|\lambda^*) \end{cases} \quad (36)$$

where,
$P(O,1|\lambda^*)$, $P(O,0|\lambda^*)$ and $P(O,-1|\lambda^*)$ are the joint probabilities for *busy*, *idle* and *fuzzy* channel state, respectively at a future time $T+1$.
The flow chart of the 3-state HMM spectrum occupancy and prediction technique for CRN is depicted in Figure 3.

4. NUMERICAL RESULTS AND DISCUSSIONS

4.1 Simulation Parameters

In this section, the performance of the 3-state HMM spectrum occupancy and prediction technique for CRN was evaluated using prediction accuracy (PA), probability of detection (PD) and spectrum utilization efficiency (SUE) through simulation in MATLAB R2022a software environment. PA determines the precision level of the outcomes of the 3-state spectrum prediction technique for the CRN. PD indicates the rate of the correctness of the detection of PU's presence when the channel spectrum is *busy* while SUE is a measure of the efficient usage of the channel bandwidth within the scarce spectrum. The comparison of the 3-state HMM with the 2-state HMM was performed with 10^4 occupancy samples in an ON and OFF manner generated using geometric distribution for each of the models while the channel of the PU follows the Poison distribution process. Table 1 presents the simulation parameters employed in this paper.

Table 1: Simulation parameters

Parameter	Specifications
Data length	10000
Bandwidth	20 MHz
Channel	Rayleigh fading channel
Noise	AWGN
Detector	Energy detector
Detection mode	Root mean square
SNR	0:2:20
ED threshold	3 dB
PFA	0.01:0.01:0.1
Modulation scheme	QAM

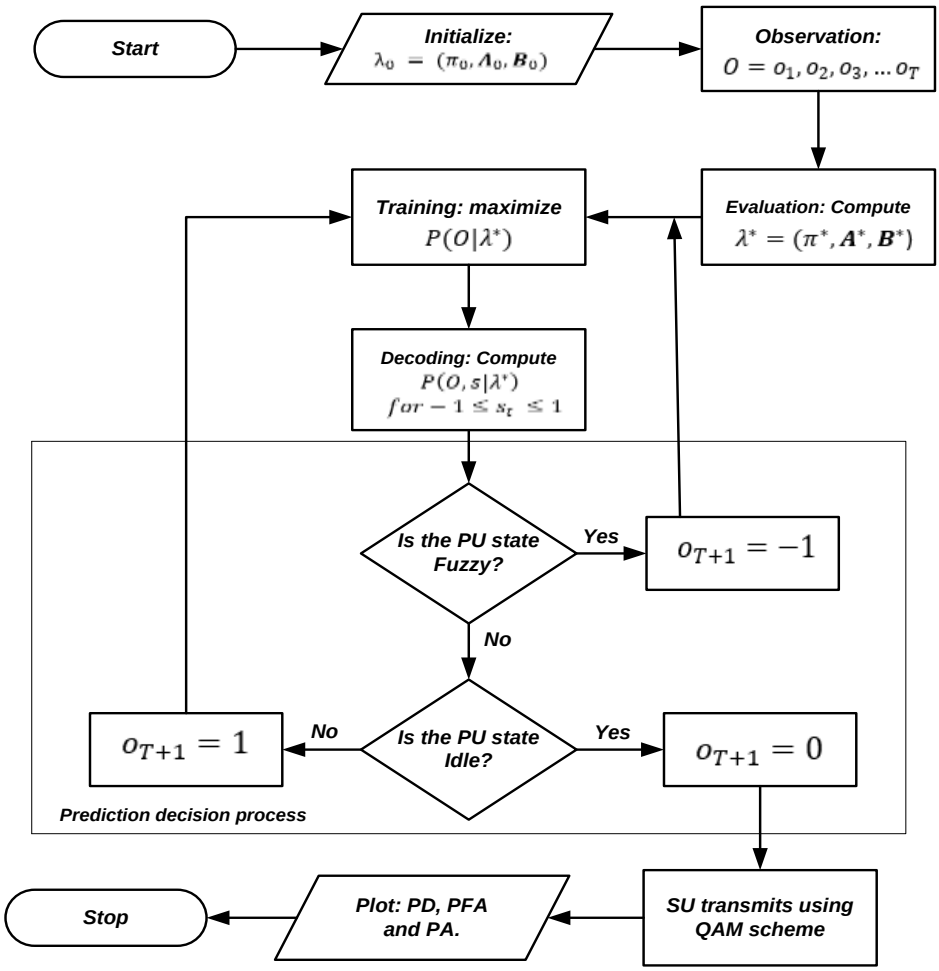

Figure 3: Flow chart of the 3-state HMM technique for CRN

4.2 Prediction Accuracy

The values of prediction accuracy obtained from the 3-state and 2-state HMM spectrum occupancy and prediction technique were plotted against varying values of SNR and PFA in Figures 4 and Figure 5, respectively. In Figure 4, PFA of 0.1 was chosen being the highest value of the decision threshold. The plot shows the value of PA increasing as the value of SNR increases for both 3-state HMM and the 2-state HMM techniques. However, at higher SNR values, the PA of the models becomes steady. At SNR of 10 dB, the accuracy value of 85.5% was recorded for the 3-state HMM while 61.7% was recorded for the 2-state HMM technique. In addition, with SNR value increased to 20 dB, the accuracy value of 99.5% and 75.4% were obtained for the 3-state HMM and the 2-state HMM techniques, respectively. This indicates that employing the 3-state HMM technique gives a better performance by reducing the errors because of the *fuzzy* state which helps to reduce the interference of the SU to the PU transmission.

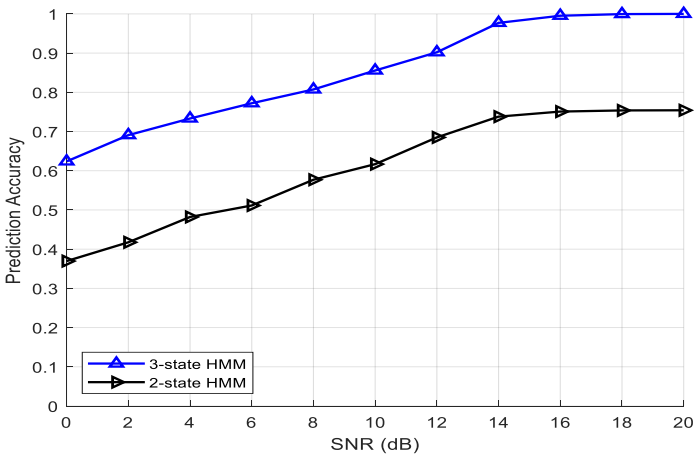

Figure 4: PA against SNR at PFA of 0.1

In Figure 5, the plot of PA against PFA is presented for the 3-state HMM technique for different fixed values of SNR. The plot revealed that the PA increases for varying values of PFA while significant improvement was recorded as the fixed value of SNR becomes higher. At a low SNR value of 6 dB, with PFA values of 0.03, 0.06 and 0.09, the PA recorded were 46.2%, 55.3% and 57.3%, respectively. With the SNR increased to 12 dB, 66.1%, 84.25% and 89.7% were obtained at 0.03, 0.06 and 0.09 values of PFA, respectively while at high SNR of 18 dB, the values of PA gave 71.2%, 92.8% and 99.3% for 0.03, 0.06 and 0.09, respectively. This result indicated that higher accuracy of the channel state of the PU can be achieved if the fuzzy state in incorporated into the 2-state HMM technique for CRN to reduce the under-utilized and scares spectrum resources.

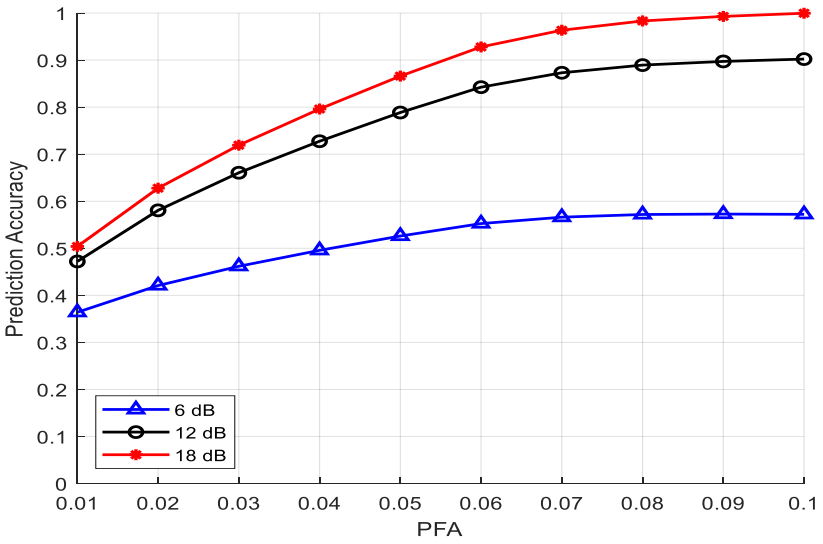

Figure 5: PA against PFA at different SNR

4.3 Probability of Detection

Figures 6 and 7 present the plots of PD against SNR and PFA, respectively. The result obtained in Figure 6 shows that as the SNR values increase, the PD of the 3-state HMM and the 2-state HMM techniques also increase at PFA of 0.1. From the result, it was observed that at low SNR value of 6 dB value, the 3-state HMM technique recorded 0.6307 as against the 2-state HMM technique with a value of 0.4721 which translates to an improvement in spectrum detection of about 25.1%. Similarly, at high SNR of 18 dB, the 3-state HMM technique recorded a detection score of 0.996 while 0.7074 was observed for the 2-state HMM technique which shows an improved detection of 29.1%. This result indicates that the 3-state HMM technique can detect the channel state correctly thereby reducing the interference that may occur because of poor detection of the PU signal.

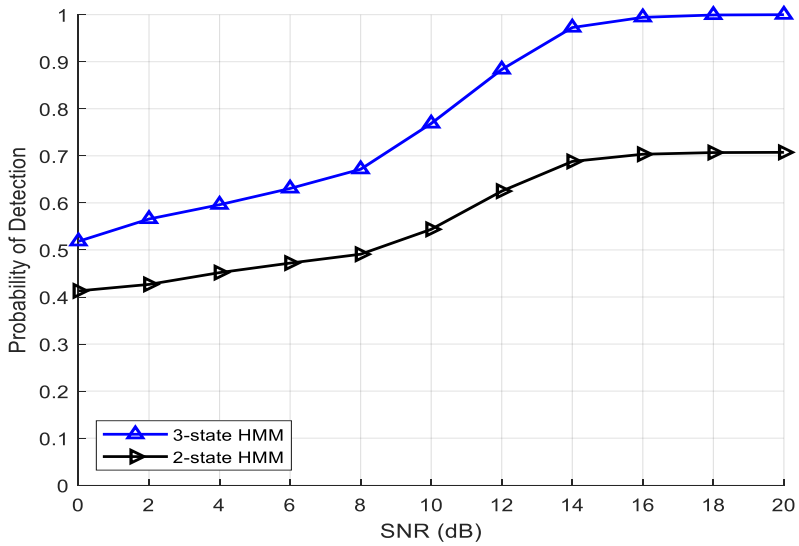

Figure 6: PD against SNR at PFA of 0.1

In Figure 7, the plot of PD against varying PFA values is drawn. The result obtained revealed that the detection increases with increase in the PFA. At a low SNR value of 6 dB, with PFA values of 0.03, 0.06 and 0.09, the PA recorded were

0.4036, 0.5718 and 0.6222, respectively. With the SNR increased to 12 dB, 0.5684, 0.8053 and 0.8764 were obtained at 0.03, 0.06 and 0.09 values of PFA, respectively while at high SNR of 18 dB with the PFAs, the values of PA gave 0.642, 0.9109 and 0.9913 for 0.03, 0.06 and 0.09, respectively. This result indicated that even at high PFA value, a better detection performance can be obtained to improve the channel occupancy state and prediction for the efficient utilization of the spectrum.

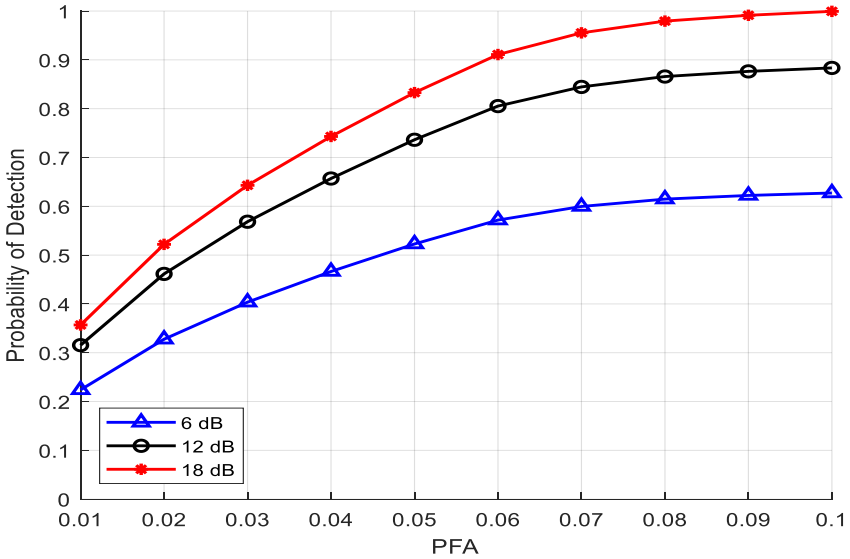

Figure 7: PD against PFA at different SNR

4.4 Spectrum Utilization Efficiency

Figures 8 and 9 present the performance of SUE against varying values of SNR and PFA, respectively. The result obtained in Figure 8 revealed that the HMM technique for CRN increases with an increase in SNR at fixed PFA of 0.1. The plot shows that at SNR of 10 dB, the SUE value of 69.6% was observed for the 3-state HMM technique while 47.7% was obtained for the 2-state HMM technique. Likewise, at SNR of 20 dB, SUE value of 83.3% was observed for the 3-state HMM technique while 51.6% was obtained for the 2-state HMM technique. This indicates that the 3-state HMM technique enhances the spectrum usage efficiently and reduces the under-utilization of the available bandwidth.

In Figure 9, the plot of SUE against PFA is drawn. The result obtained revealed that the usage of the spectrum increases with an increase in the PFA value. At a low SNR value of 6 dB, with PFA values of 0.03, 0.06 and 0.09, the SUE values of 49.6%, 51.6% and 57.1% were obtained, respectively. With the SNR increased to 12 dB, 58.8%, 69.3% and 73.4% were obtained at 0.03, 0.06 and 0.09 values of PFA, respectively while at high SNR of 18 dB at PFA of 0.03, 0.06 and 0.09, the values of SUE gave 62.7%, 76.5% and 82.6%, respectively. This result indicated that with high value of PFA, the spectrum usage performance is significantly utilized making the 3-state HMM technique for CRN channel occupancy and prediction more robust and suitable for deployment in emerging networks.

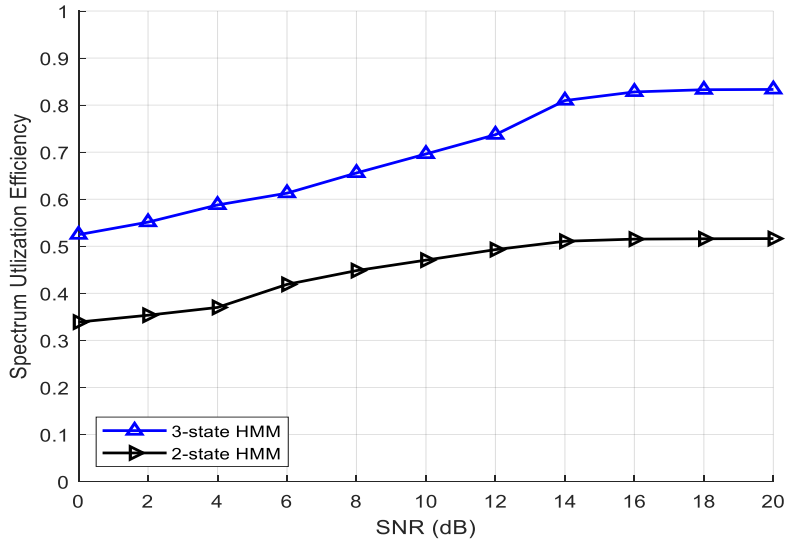

Figure 8: SUE against SNR at PFA of 0.1

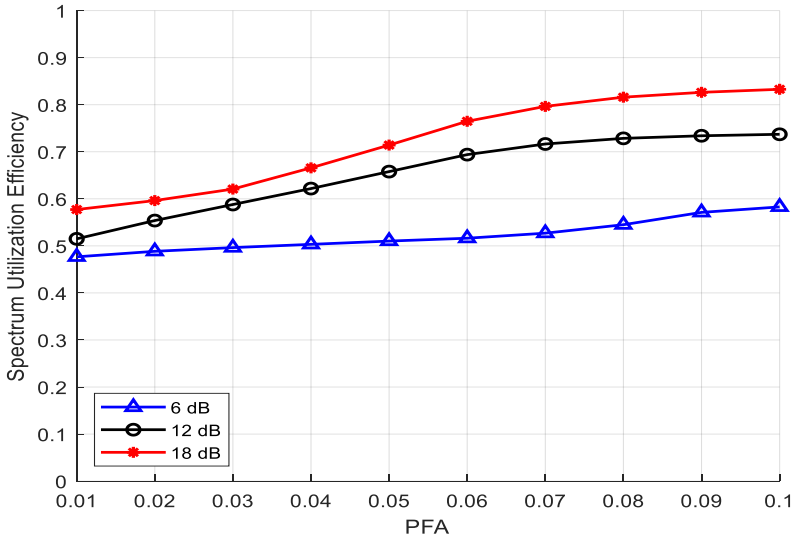

Figure 9: SUE against PFA at different SNR

5. CONCLUSION

This paper has proposed spectrum prediction technique in CRNs using 3-state HMM. The 3-state HMM is formulated from the 2-state model. The formulation involved a doubly stochastic process which combined an observable process and a hidden process. Expressions are derived for the initial state probability, the observation symbol probability distribution in each state and the state transition probability distribution in a 3-state HMM. The three canonical problems peculiar with HMM are solved for the proposed model to be suitable in real-network applications using forward and backward, Viterbi and Baum-Welch algorithms. The three hidden states identified in practical scenarios were "*idle*", "*busy*" and "*fuzzy*" states. The results obtained reveal that the 3-state spectrum prediction technique gives a better performance with improved prediction accuracy, probability of detection and spectrum utilization efficiency over the 2-state HMM. The outstanding performance of the proposed model was due to the *fuzzy* state incorporated in the development of the model. Consequently, the 3-state spectrum prediction technique has reduced both the interference to PU and false alarm in CRNs as well as reduce the wastage of resources.

REFERENCES

[1] Goldon, L.S. (2017). *Principles of Mobile Communications*. 4th ed., Cham, Switzerland.
[2] Akyildiz, I.F., Su, W., Sankarasubramaniam, Y., & Cayirci, E. (2002). Wireless sensor networks: a survey. Computer Networks, 38(2), 393–422.
[3] Akande, D.O., Adeyemo, Z.K., Arowolo, O.O., Oseni, O.F. & Obanisola, O.O. (2022). Hybridization of zero forcing-minimum mean square error equalizer in multiple-input multiple-output system. Indonesian Journal of Electrical Engineering and Computer Science, 26(2), 836-845.
[4] Mitola, J. (2000). Cognitive radio: an integrated agent architecture for software defined radio. PhD Thesis, Royal Institute of Technology. 271-350.
[5] Annapurna, K., Hymavathi, T., & Ramanjaneyulu, B.S. (2019). Spectrum availability prediction for cognitive radio networks. International Journal of Recent Technology and Engineering. 7(54), 257–260.
[6] Tandra, R., Mishra, S.M., & Sahai, A. (2009). What is a spectrum hole and what does it take to recognize one?. Proceedings of the IEEE Journals and Magazine, 97(5), 824–848.
[7] Nur, S.H., Mas, H.M., & Aduwati, S. (2021). Sensing and analysis of spectrum holes in ISM band using USRP testbed. TELKOMNIKA Telecommunication, Computing, Electronics and Control, 19(6), 1761-1768.
[8] Ojo, S.I., Adeyemo, Z.K., Akande, D.O., & Fawole, A.O. (2021). Energy-efficient cluster-based cooperative spectrum sensing in a multiple antenna cognitive radio network. International Journal of Electrical and Electronic Engineering and Telecommunications, 10(3), 176-185.
[9] Chintha, T & Sachita, K., (2017). An overview of cognitive radio networks. J. Webster (ed.), Wiley Encyclopedia of Electrical and Electronics Engineering. John Wiley & Sons, Inc.
[10] Kolodzy, P., (2001). Next generation communication: kick off meetings. Proceedings of Defense Advanced Research Projects Agency, Airlington. 388.
[11] Ding, G., Jiao, Y.W., Zou, Y., Wu, Q., Yao, Y.D., & Hanzo, L., (2017). Spectrum inference in cognitive radio networks: algorithms and applications", IEEE Communications Surveys and Tutorials.1–34.
[12] Anirudh, A., Aditya, S., & Ranjan, G., (2018). Spectrum occupancy prediction for realistic traffic scenarios: time-series versus learning-based models. Journal of Communications and Information Networks, 1-18.

[13] Sayhia, T., & Zoheir, H., (2019). A survey on spectrum prediction methods in cognitive radio networks", International Journal of Computing Academic Research, 8(2), 24–31.
[14] Jianwei, W., & Yanling, L., (2017). A survey of spectrum prediction methods in cognitive radio networks", AIP Conference Proceedings. 17(1834), 1–5.
[15] Acharya, P.A.K., Singh, S., & Zheng, H. (2006). Reliable open spectrum communications through proactive spectrum access. Proceedings of the First International Workshop on Technology and Policy for Accessing Spectrum. 5–12.
[16] Zhang, X., Guo, L., Ben, C., Peng, Y., Wang, Y., Shi, S., Lin, Y.& Gui, G., (2024). A-GCRNN: Attention graph convolution recurrent neural network for multi-band spectrum Prediction. IEEE Transactions on Vehicular Technology. 73(2), .2978-2982.
[17] Sumithra, M. G., & Suriya, M., (2024). Improved spectrum prediction model for cognitive radio networks using hybrid deep learning technique. International Journal of Intelligent Networks. 5:286-292.
[18] Tumuluru, V., Wang, P., & Niyato, D. (2012). Channel status prediction for cognitive radio networks. Wireless Communications and Mobile Computing. 12(10), 862-874.
[19] Anirudh, A., Shivangi, D., Mohd, A.K., Ranjan, G., & Soumitra, D. (2016). Learning based primary user activity prediction on cognitive radio networks for efficient dynamic spectrum access. International Conference on Signal Processing and Communications. 1-5.
[20] Ramiyar, H., Shahpour, A., Arash, A., Majid, A., & Iman, M., (2015). Primary user activity prediction using the hidden Markov model in cognitive radio networks. International Symposium on Signals. Circuits and Systems, 1-4.
[21] Jaison, J., Babita, R.J., and Jimson, M., (2014). Spectrum Prediction in Cognitive Radio Networks: A Bayesian Approach. International Conference on Next Generation Mobile Apps, Services and Technologies, 14(8), 203–208.
[22] Tumuluru, V., Wang, P., & Niyato, D. (2010). A neural network-based spectrum prediction scheme for cognitive radio", IEEE International Conference on Communications. 1–5.
[23] Eleftherios, C. (2014). Spectrum sensing and occupancy prediction for cognitive machine-to-machine wireless networks. PhD Thesis. University of Bedfordshire. Luton. England, 2014.
[24] Saad, A., Staehle, B., & Knorr, R. (2016). Spectrum prediction using hidden Markov models for industrial cognitive radio, IEEE 12th International Conference on Wireless and Mobile Computing, Networking and Communications. 1-7.
[25] Zhe, C. & Robert, C.Q. (2010). Prediction of channel state for cognitive radio using higher-order hidden Markov model. Proceedings of the IEEE South-east Conference, Concord, NC, USA. 276-282.
[26] Wang, J., & Adriman, R. (2015). Analysis of opportunistic spectrum access in cognitive radio networks using hidden Markov model with state prediction. EURASIP Journal on Wireless Communications and Networking. 10. 2-8.
[27] Abramowitz, M., & Stegun, I.A. (1972). *Handbook of mathematical functions: with formulas, graphs, and mathematical tables*. Courier Dover Publications.
[28] Rabiner, L.R. (1989). A Tutorial on hidden Markov models and selected applications in speech recognition", Proceedings of the IEEE Journals and Magazines. 77(2), 257–286.